Effects of Polymer Layer Anisotropy on the Interaction between Adsorbed Layers

Murali Rangarajan, Jorge Jimenez,† and Raj Rajagopalan*

Departmet of Chemical Engineering, University of Florida, Gainesville, Florida 32611

Received August 3, 2001; Revised Manuscript Received March 25, 2002

ABSTRACT: We examine the effects of polymer layer anisotropy (bond correlations) on the numerical mean-field predictions of the interactions between two physisorbed polymer layers under restricted equilibrium conditions. Lattice mean-field calculations are presented for two models based on second-order Markov chains (i.e., without backfolding), one in an isotropic mean field and another in an anisotropic mean field. The results from lattice Monte Carlo simulations are used as a reference to examine those obtained from the numerical mean-field theories. It is found that the numerical mean-field theories predict the structural features of the polymer layer fairly well but are limited in the predictions of the interaction forces. The effects of anisotropy near and away from the adsorbing surface differ from each other but are still insufficient to capture the interactions accurately. Introduction of anisotropy results in higher segment densities of trains but lower segment densities of loops, tails, and bridges and, consequently, lower steric interactions. It is seen that the mean-field theories can at best offer qualitative information on the structure of the adsorbed layer and of the interaction forces at conditions where steric interactions become important (at high coverages). At conditions where bridging interactions dominate (at low coverages), the mean-field theories fail to capture the bridging attraction between the surfaces (as expected), in contrast to some of the earlier published reports.

1. Introduction

Polymer adsorption is of great importance in various processes of technological and biological relevance (e.g., stabilization of colloidal suspensions, adhesion, lubrication, bilayer membranes, etc.). To have an effective understanding and control over any of these processes, it is important to understand the static and dynamic properties of the adsorbed layers. A model case that has been investigated widely is the adsorption of linear, flexible polymers onto one or two uniform flat surfaces[1]. The structure of the adsorbed polymer layer is described in terms of trains, loops, and tails—and additionally in terms of bridges in the case of two interacting layers. The primary purpose of theoretical attempts in this area is to develop predictive equations for the structure of the layers and to relate the structure to the forces.

Two groups of theories, commonly referred to as "scaling theories" and "mean-field" theories, are commonly used in the literature to provide guidelines on the structure of the adsorbed polymer layer and polymer-induced forces and to interpret experimental results. The mean-field theories can be analytical or can be implemented numerically on a lattice. Analytical mean-field theories for the study of polymer adsorption are based on the pioneering works by Edwards[2] and de Gennes[3,4] (ground-state-dominance approximation). Dolan and Edwards[5] applied the mean-field theory to the interactions between polymer bearing surfaces. Recently Semenov and co-workers[6,7] extended the ground-state-dominance approximation to include another order parameter, to account for the effects of chain ends. Bonet-Avalos et al.[8] have used this so-called two-order-parameter theory to estimate the forces between two polymer layers in "full equilibrium" with a bulk solution, while Mendez-Alcaraz et al.[9] have studied the case of two polymer layers in "restricted equilibrium" with its surroundings. (An explanation of "full equilibrium" and "restricted equilibrium" is provided in the next section.) The numerical mean-field theories would include the commonly used Scheutjens and Fleer's lattice mean-field theory [10,11,12] and its variations.[13] The scaling theory of polymer adsorption (Rossi and Klein,[14] and references therein) is based on the minimization of the surface free energy functional that is similar in form to the free energy functional considered in the ground-state-dominance approximation and other earlier analytical mean-field treatments of the problem (Edwards[2] and Jones and Richmond[15]). However, the dependence of the free energy on segment volume fraction is chosen in such a way as to reproduce the scaling laws under good solvent conditions. These theories have been used to obtain simple scaling relationships for the structure of the adsorbed layer and the interaction forces in the asymptotic limit of infinite molecular weight (analytical mean-field theories and scaling theories) and also for short chains (numerical mean-field theories).

The Dutch group has made a comprehensive attempt to understand many problems on polymer adsorption such as interaction between two adsorbed polymer layers, terminally grafted chains, ring polymers, branched chains, block and random copolymers and polyelectrolytes (see Fleer et al.[13] for more details and references). The original Scheutjens and Fleer [10,11,12] formulation for the study of simple, homopolymer adsorption is based on first-order Markov chain statistics. In this paper, this formulation will be referred to as SF_1. Two important improvements on SF_1 have been proposed, one being the formulation to exclude immediate backfolding of segments in a chain.[16] This formulation considers the polymer chains as second-order Markov chains and therefore excludes the overlapping of sequential segments. It will henceforth be referred to as SF_2 in this paper. Both SF_1 and SF_2 consider an isotropic mean

* To whom correspondence should be addressed. E-mail: raj@che.ufl.edu.

† Present address: The Dow Chemical Co., 2301 N. Brazosport Blvd., B-1225, Freeport, TX 77541-3257.

10.1021/ma011395p CCC: $22.00
Published on Web 06/19/2002

field. The other improvement of interest is the introduction of anisotropy in the mean field by partially accounting for the effects of bond orientations on the equilibrium properties of the system. The self-consistent anisotropic mean-field theory (SCAFT) was first proposed by Leermakers and Scheutjens[17] to study phase transitions in lipid bilayer membranes, to account for the anisotropic orientational interactions between the lipidlike molecules in a membrane. The theory was able to successfully predict the critical phase behavior of the membrane observed in experiments. This work also provided an elegant derivation of the theory from the basic principles of statistical thermodynamics. Recently, van der Linden et al.[18] extended the Scheutjens and Fleer theory to semiflexible polymers, in which bond correlations were incorporated. In both these works, the authors studied only the overall segment densities and some of the broad structural features. The focus in the former work was to develop a theory for membranes based on statistical thermodynamics and that of the latter work was to formulate a lattice mean-field theory for semiflexible polymers (e.g., "wormlike" chains). Fleer et al.[19,20] have attempted to relate the numerical mean-field formalism and the two-order-parameter theory in an attempt to obtain closed-form solutions that reproduce the numerical mean-field results.

The numerical mean-field theory of Scheutjens and Fleer is, presently, the only theory from which one can obtain quantitative guidelines on the adsorption of short chains (of finite molecular weight). It is therefore important to ascertain the reliability of this theory in predicting the structural details of the adsorbed layer, and the forces of compression of two polymer layers. Comparisons have been made with experiments in the literature (e.g., Fleer et al.[13]). However, many of the intricate structural details of the adsorbed layer are either inaccessible or not easily accessible through experiments, such as specific information on loops, tails, and bridges. Moreover, experiments involve many parameters that cannot be precisely controlled or do not factor into most theories, such as surface roughness and polydispersity of the polymer. Another very important issue in comparisons with experiments is the ambiguity in relating a theoretical state of the system (as defined by the number of chains, number of Kuhn units, a theoretical adsorption energy, and a theoretical segment−solvent interaction (χ) parameter) with appropriate experimental conditions. These considerations limit the extent of any such comparison to one of *qualitative* nature. In view of these, while it may be instructive and important to assess the validity of a theory against experiments, a simple, direct comparison would not only be limited but also, under most conditions, be misleading. On the other hand, computer simulations are "exact" within their approximations (e.g., lattice approximation in lattice MC simulations), and comparisons against lattice-based simulations would enable one to assess the limitations of the mean-field approximation in the context of lattice mean-field theories. We, therefore, use Monte Carlo results[21] of realistic chains (self-avoiding walks), *within the lattice formalism* as a reference, to examine the predictions of the mean-field theories.

In the present work, we consider the effects of anisotropy in the layer on the resulting mean-field predictions of the structure of the layer as well as the forces arising from the interactions between two layers. Specifically, we introduce anisotropy in the SF_2 formulation. We also provide preliminary comparisons of the anisotropic mean-field predictions of the structure of the adsorbed layers against results from rigorous computer simulations.[21] A summary of the anisotropic mean-field formulation is provided in the next section. (Further details are available elsewhere; see Fleer et al.[13] and Leermakers and Scheutjens.[17]) We then discuss the improvements in the predictions due to the introduction of anisotropy and comment on the limitations of mean-field theories as seen from these comparisons. One of our objectives in the next section is to present a clear and easily understandable anisotropic mean-field formulation and to provide expressions for the various structural features of the adsorbed polymer layer.

2. Self-Consistent Anisotropic Mean-Field Theory (SCAFT)

2.1. Preliminaries and Notations. Consider a lattice system confined between two flat, parallel, impenetrable surfaces and filled with polymer segments (chains of finite length, r) and solvent molecules. We only consider fluctuations in a single direction normal to the surface, which we define as the z-direction. Each segment or solvent molecule occupies one lattice site. The lattice adjoins one or two hard/adsorbing surfaces and is divided into M layers of sites parallel to the adsorbing surfaces, in the z-direction. Each layer contains L lattice sites. The surfaces therefore correspond to $z = 0$ and $z = M + 1$, and adsorption takes place in $z = 1$ and $z = M$. If D is the coordination number of the lattice, then a lattice site in any layer z has D nearest neighbors, of which a fraction $\lambda_{z'-z}$ is in layer z'. The fraction of nearest neighbors that lie in the same layer, then, is λ_0, and that in the adjacent layer is λ_1 and so on. Therefore, λ can be viewed as the fraction of the nearest neighbors of a lattice site. In the case of a first-order Markov chain statistics, λ's are the step-weights of the random walk. Furthermore, in a simple cubic lattice, there are six nearest neighbors to a lattice site in a layer z, of which four are in layer z and one each in the layers $z \pm 1$. Therefore, for a cubic lattice, $\lambda_{\pm 1} = {}^1/_6$, $\lambda_0 = {}^4/_6$, and, $\lambda_{\pm j} = 0$, $|\, j \,| > 1$. If there are n polymer chains and n^0 solvent molecules between the surfaces, then it follows that

$$nr + n^0 = ML \tag{1}$$

We define the volume fractions of polymer and solvent at any given layer as

$$\phi(z) = \frac{n(z)}{L}; \quad \phi^0(z) = \frac{n^0(z)}{L} \tag{2}$$

such that

$$n(z) + n^0(z) = L; \quad \phi(z) = 1 - \phi^0(z) \tag{3}$$

and

$$\sum_z n(z) = nr; \quad \sum_z n^0(z) = n^0 \tag{4}$$

One can distinguish three possibilities in such a system.

1. When the characteristic time of compression of the layer is larger than that of desorption, the chemical potentials of the polymer chains and solvent molecules are the same as the corresponding ones in the "sur-

rounding" bulk solution. This situation is referred to as the *full equilibrium* situation. To maintain the constant chemical potential, the total amount of polymer between the surfaces varies as the system is compressed.

2. The solvent is in equilibrium with the bulk solution whereas the total amount of polymer in the system is fixed. This would correspond to a case when the characteristic time for desorption of polymer chains is larger than the characteristic time of compression. If the characteristic time for rearrangement of the conformations is significantly smaller than the time of compression, the solvent molecules "drain" out while the polymer chains (whose total mass is fixed) between the surfaces rearrange themselves into new "equilibrium" conformations. This situation is referred to as *restricted equilibrium*.

3. The third possibility would correspond to the case in which the polymer chains take longer time to rearrange themselves than the time taken to compress the system. Then, the chains would not have reached equilibrium with the bulk solution. This is the *nonequilibrium* case.

We now present the relevant equations for the case of *restricted equilibrium*. The polymer chains are modeled as step-weighted random walks in a simple cubic lattice. We consider second-order Markov chain statistics in which immediate step-reversals (backfolding of segments) are disallowed. The dimensionless mean-field potential $u(z)$ that a polymer segment experiences in layer z is given as

$$u(z) = -\chi_{s1}\delta_{1z} - \chi_{sM}\delta_{Mz} + u^{\text{int}}(z) + u'(z) \qquad (5)$$

where χ_{si} is the Silberberg adsorption energy parameter for the polymer/solvent pair on the surface at layer z and δ_{ij} is the standard Kronecker delta function. The term $u^{\text{int}}(z)$ accounts for the energetic interactions between the polymer segments and solvent molecules within the Bragg−Williams random mixing approximation

$$u^{\text{int}}(z) = \chi\,[\langle\phi(z)\rangle - \langle\phi^{0}(z)\rangle] \qquad (6)$$

Here, χ is the Flory−Huggins segment−solvent interaction parameter that decides the solvent quality. In the present work, we examine only good solvent conditions, for which $\chi = 0$. The near-neighbor average of volume fraction of the segments in layer z is given by

$$\langle\phi(z)\rangle = \sum_{z'=1}^{M} \lambda_{z'-z}\phi(z') \qquad (7)$$

which, for a cubic lattice with only the nearest-neighbor interactions, becomes

$$\langle\phi(z)\rangle = \lambda_{-1}\phi(z-1) + \lambda_0\phi(z) + \lambda_1\phi(z+1)$$

The Lagrange parameter $u'(z)$ in eq 5 partially accounts for the excluded volume of the segment and solvent in a given layer. This is usually based on the Bragg−Williams random-mixing approximation.

2.2. Anisotropic Mean Field. Anisotropic mean-field theory attempts to improve upon the Bragg−Williams approximation in order to better account for the excluded volume. To better understand the idea of anisotropic mean-field, let us consider a polymer chain as a set of segments connected by bonds of defined

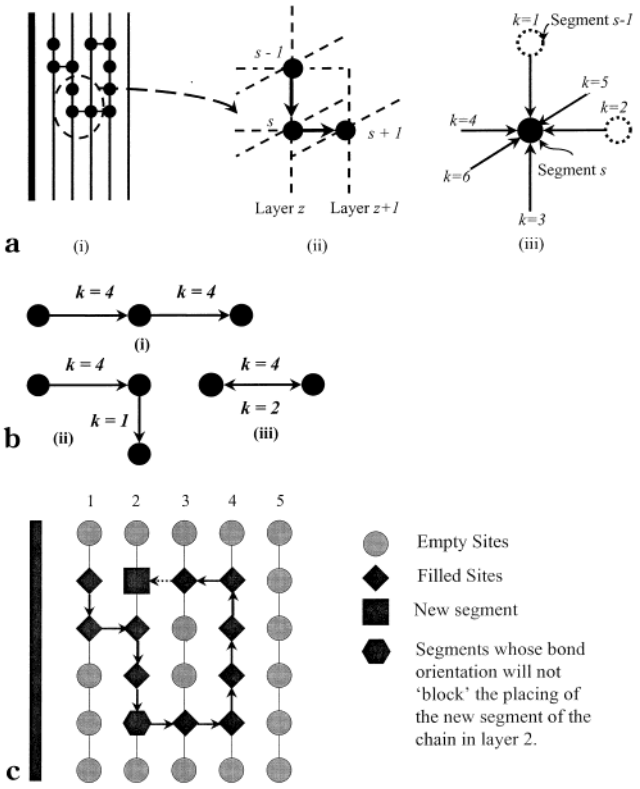

Figure 1. (a) Notion of bond orientations: (i) typical polymer chain in a lattice; (ii) segments and bonds; (iii) bond orientations. In the illustration above, the orientation of the bond between segment $(s-1)$ and segment s (in part ii) is $k = 1$ (see part iii). This way of representing bond orientation thus indirectly specifies the position of the previous, e.g., $(s-1)$th, segment. In a cubic lattice there are six possible orientations. These six orientations can be thought of as three pairs of "opposite" orientations. For instance, $k = 1$ and $k = 3$ are "opposite" orientations. Consecutive segments with "opposite" orientations will cause a backfolded conformation. (b) Conformations of consecutive bonds: (i) straight; (ii) perpendicular; (iii) backfolded. (c) Schematic representation of the anisotropic mean field in a square lattice: isotropic mean field, probability of placing a new segment in layer 2 = $^3/_6$; anisotropic mean field, probability of placing a new segment in layer 2 = $^3/_5$.

orientations. The notion of bond orientations is illustrated in Figure 1a. Between any three consecutive segments, three conformations can be identified: namely, a straight conformation, a perpendicular conformation, and a backfolded conformation. These conformations are illustrated in Figure 1b. Second-order Markov chain statistics do not allow the physically unrealistic backfolded conformation. In the case of isotropic mean field, the excluded volume is accounted for by just requiring that the probability of having a segment in a layer is the fraction of empty sites in that layer. (This is the standard Bragg−Williams random mixing approximation.) Therefore, all the bond orientations are equally likely (within the restrictions imposed by the chain statistics). In an anisotropic mean field, the orientation of a polymer segment in a given layer depends on the orientations of its neighboring segments (the neighboring bonds), which a priori limit the probability of having the segment in that layer. This is illustrated in Figure 1c. This therefore means that each orientation has to be weighted appropriately. This introduces a bias in the step-weights of the random walk, making the mean field anisotropic.[22] This idea is explained further below.

In an isotropic mean field, the Lagrange parameter $u'(z)$ is given by the fraction of "empty" lattice sites in the layer z, which is equivalent to the volume fraction of solvents (for "good" solvents).

$$u'(z) = \ln(1 - \phi(z)) \tag{8}$$

In the case of anisotropic mean field, there are a priori fewer "empty" sites available in the layer z once we account for the fact that those segments in layer z with the same bond orientation and those in layer $z \pm 1$ with a complementary orientation will not "block" the given bond orientation. Let $\Omega(z, k)$ be the fraction of bonds with those orientations that will not block a bond with an orientation k.

$$\Omega(z, k) = \sum_{s} \{\phi(z, s, k) + \phi(z', s, k')\} \tag{9}$$

Here, k and k' are "opposite" bond orientations (see Figure 1c), and $z' = z$ or $z \pm 1$, as the case may be. $\phi(z, s, k)$ is the volume fraction of sth segments (in r-mers) with a bond orientation k, in layer z. Therefore, $1 - \Omega(z, k)$ is the maximum available fraction of "empty" sites in layer z for a segment to occupy with a bond orientation k.

This correction factor is given as

$$g(z, k) = \frac{1}{1\text{-}\Omega(z, k)} \tag{10}$$

where $\Omega(z, k)$ is the fraction of bonds with those orientations that will not block a bond with an orientation k. Note that in the case of isotropic mean field, the correction factor is unity.

2.3. Statistical Weights and Composition Rule. The Boltzmann factor

$$G_m(z) = \exp\left(-\frac{u(z)}{k_B T}\right) \tag{11}$$

defines the so-called free/monomer segment distribution function. It is evidently the unnormalized probability of a "monomer" segment in layer z. We now define the unnormalized probability[23] $G(z, s, k)$, of a s-mer, with the end-segment located in layer z, with a bond orientation k (as per the definition of bond orientations in Figure 1a). Since we model the chain using Markov statistics, the probability of a s-mer can be obtained by summing the probabilities of adding a monomer to the different possible orientations of a $(s - 1)$-mer that will give rise to the desired conformation (defined by $G(z, s, k)$), thereby resulting in a recursive relation for evaluating the statistical weights. To be consistent with the notation, we need to define the monomer statistical weights as $G(z, 1, k)$ even though bond orientations do not have a physical meaning in this case. For a cubic lattice, we therefore write

$$G(z, 1, k) = \frac{G_m(z)}{6} \tag{12}$$

The corrections for the anisotropy due to bond orientations should be introduced from dimers on. We now write the statistical weights for dimers.

$$G(z, 2, k) = G_m(z)\, g(z, k) \sum_{l=1}^{6} G(z', 1, l) \tag{13}$$

Using second-order Markov statistics, we can further write the statistical weights of a s-mer as

$$G(z, s, k) = G_m(z)\, g(z, k) \sum_{l \neq k'} G(z', s - 1, l) \tag{14}$$

To introduce a short-hand notation, we write the above equations as

$$G(z, s, k) = G_m(z) g(z, k) \langle G(z', s - 1, l) \rangle \tag{15}$$

Note that this way of evaluating the statistical weights automatically ensures chain connectivity as shown by Scheutjens and Fleer.[10] We now proceed to evaluate the segment volume fractions (which we call segment densities) using the so-called *composition rule*

$$\phi(z, s, k) = C \frac{G(z, s, k) \sum_{l \neq k} G(z, r-s+1, l)}{(5/6) G_m(z)}, \quad \text{if } s \neq 1 \text{ or } r \tag{16}$$

$$\phi(z, s, k) = C \frac{G(z, s, k) \sum_{l=1}^{6} G(z, r-s+1, l)}{G_m(z)}, \quad \text{if } s = 1 \text{ or } r \tag{17}$$

$$\phi(z) = \sum_{s=1}^{r} \sum_{k=1}^{6} \phi(z, s, k) \tag{18}$$

Here, C is a normalization constant to account for the fact that the statistical weights are not normalized. For the case of *restricted equilibrium*, it is defined as

$$C = \frac{\theta^t}{r G(r)} = \frac{n}{L G(r)} \tag{19}$$

where θ^t is the total amount of polymer between the plates and $G(r)$ is the so-called end-segment distribution, i.e., the statistical weight of finding a r-mer anywhere between the two surfaces. The former is defined as

$$\theta^t = \sum_{z} \phi(z) = \frac{nr}{L} \tag{20}$$

and the latter is defined as

$$G(r) = \sum_{z=1}^{M} \sum_{k=1}^{6} G(z, r, k) \tag{21}$$

A self-consistent solution is obtained by assuming a density profile and isotropic mean field (as initial guess) and using an iterative procedure to evaluate the volume fractions.

2.4. Structure of the Adsorbed Layer. Once a self-consistent solution is obtained for the segment densities, one can easily obtain details of the structure of the adsorbed layer and the free energy of the system. To do this, we see that the polymer chains between the two surfaces (θ^t) are in one of the five following groups:[24]

1. The chains are free, θ^f.
2. The chains are adsorbed only to surface "1", θ_1^a.
3. The chains are adsorbed only to surface "2", θ_2^a.

4. The chains form bridges, with the last chain end leaving from surface "1", θ_1^b.

5. The chains form bridges, with the last chain end leaving from surface "2", θ_2^b.

Therefore, we have

$$\theta^t = \theta^f + \theta_1^a + \theta_2^a + \theta_1^b + \theta_2^b \tag{22}$$

Since $\theta^t = CrG(r)$, we define,

$$G(r) = G^f(r) + G_1^a(r) + G_2^a(r) + G_1^b(r) + G_2^b(r) \tag{23}$$

and further,

$$G^*(r) = \sum_{z=1}^{M} \sum_{k=1}^{6} G^*(z, r, k) \tag{24}$$

for each of the groups (represented by $*$). Now we proceed to define recursive relationships for the statistical weights of free, adsorbed and bridged chains similar to the way we defined the statistical weights before.

Free Chains. Since free chains cannot have a segment in layers 1 or M, we have

$$G^f(z, 1, k) = \begin{cases} G(z, 1, k), & \text{if } 1 < z < M \\ 0, & \text{if } z = 1 \text{ or } M \end{cases} \tag{25}$$

$$G^f(z, s, k) = G_m(z)\, g(z, k)\, \langle G^f(z', s-1, l)\rangle \tag{26}$$

subject to the conditions

$$G^f(z, s, k) = 0, \quad \text{for all } s, \text{ if } z = 1 \text{ or } M \tag{27}$$

Adsorbed Chains. We define similar expressions for adsorbed chains as for free chains. For instance, the statistical weight of a chain adsorbed to surface "1" is given by

$$G_1^a(z, 1, k) = \begin{cases} G(z, 1, k), & \text{if } z = 1 \\ 0, & \text{otherwise} \end{cases} \tag{28}$$

$$G_1^a(z, s, k) = G_m(z) g(z, k)\, \langle G_1^a(z', s-1, l)\rangle, \quad \text{if } z \neq 1,\ k \neq 2 \tag{29}$$

$$G_1^a(1, s, 2) = \frac{G_m(1) g(1, 2)}{5} \sum_{l \neq 4} \{G_1^a(2, s-1, l) + G^f(2, s-1, l)\} \tag{30}$$

subject to the conditions

$$G_1^a(M, s, k) = 0;\ G_1^a(1, s, 4) = 0, \quad \text{for all } s, k \tag{31}$$

In equation 31, the term $G_m(1)\, g(1, 2) \sum_{l \neq 4} G^f(2, s-1, l)$ would occur in the recursive expression for $G^f(1, s, 2)$ according to the notation. However, it actually corresponds to conformations of s-mers with only the end segment adsorbed. Hence it is added to $G_1^a(1, s, 2)$.

Bridged Chains. The recursive relations for bridged chains are very similar to those for the adsorbed chains. For instance, the statistical weight of a chain forming a bridge with the last chain end leaving surface "1" is given by

$$G_1^b(z, 1, k) = 0, \quad z > 1 \tag{32}$$

$$G_1^b(z, s, k) = G_m(z) g(z, k) \langle G_1^b(z', s-1, l)\rangle, \quad \text{if } z \neq 1,\ k \neq 2 \tag{33}$$

$$G_1^b(1, s, 2) = \frac{G_m(1) g(1, 2)}{5} \sum_{l \neq 4} \{G_1^b(2, s-1, l) + G_2^b(2, s-1, l) + G_2{}^a(2, s-1, l)\} \tag{34}$$

subject to the conditions

$$G_1^b(M, s, k) = 0;\ G_1^b(1, s, 4) = 0, \quad \text{for all } s, k \tag{35}$$

Again, the terms $G_m(1)\ g(1, 2) \sum_{l \neq 4} G_2^b(2, s-1, l)$ and $G_m(1) g(1, 2) \sum_{l \neq 4} G_2^a(2, s-1, l)$ would occur in the recursive expressions for $G_2^b(1, s, 2)$ and $G_2^a(1, s, 2)$, respectively. However they actually correspond to bridged chains with the last chain end at surface "1". Hence they are added to $G_1^b(1, s, 2)$.

Now the segment densities of adsorbed chains and bridged chains are found by writing similar composition rules. As an example, the volume fraction of the segments which form tails from surface "1" is given by

$$\phi_1^{a,t}(z) = 2\, C \sum_{s=1}^{r} \sum_{k=1}^{6} \frac{G_1^a(z, s, k) \sum_{l \neq k} G^f(z, r-s+1, l)}{G_m(z)} \tag{36}$$

Since a chain has two ends, the prefactor 2 is added to the equation.

Once we have the statistical weights of free, adsorbed, and bridged chains, we can also estimate the average number and sizes of loops, tails, trains, and bridges. Details of these are provided in Scheutjens and Fleer's paper.[12] To give an illustration, we consider the average number and size of loops. In a loop, both the ends are adsorbed on the same surface. Therefore, we consider the *statistical weight of an adsorbed r-mer having the segment s in layer "2" and the segment* $s+1$ *in layer "1" (adsorbed), with the r-mer adsorbed at least once before segment s*. This is equal to the product $G_1^a(2, r-s+1, 4) \sum_{k \neq 4} G_1^a(2, s, k)$. We normalize the statistical weight with the *statistical weight of an adsorbed r-mer* to obtain the probability of finding an adsorbed r-mer having the segment s in layer "2" and the segment $s+1$ in layer "1" (adsorbed), with the r-mer adsorbed at least once before segments. This will be equal to the *fraction of adsorbed chains with loops ending in segment s*. Summing over all the possible values of s gives the *average number of loops per adsorbed chain*, n_l. The average number of loops per adsorbed chain (adsorbed on surface "1") $n_{1,l}^a$ is then given by

$$n_{1,l}^a = \frac{\sum_{s=3}^{r-1} \{G_1^a(2, r-s+1, 4) \sum_{k \neq 4} G_1^a(2, s, k)\}}{G_1^a(r) G_m(2)} \tag{37}$$

$$G_1^a(r) = \sum_{z=1}^{M} \sum_{k=1}^{6} G_1^a(z, r, k) \tag{38}$$

The average size of the loops in the chains adsorbed on surface "1" $l_{1,l}^a$ is then given by

$$l^{a}_{1,l} = \frac{\zeta^{a}_{1,l}}{n^{a}_{1,l}} \tag{39}$$

where $\zeta^{a}_{1,l}$ is the fraction of loops and θ^{a}_{1} is the amount of polymer adsorbed on the surface "1", and they are given by

$$\zeta^{a}_{1,l} = \frac{\sum_z \phi^{a}_{1,l}(z)}{\theta^{a}_{1}} \tag{40}$$

$$\theta^{a}_{1} = \phi^{a}_{1,tr} + \sum_z \{\phi^{a}_{1,l}(z) + \phi^{a}_{1,ta}(z)\} \tag{41}$$

Loops are formed on surface "1" by chains in groups "2" and "4", i.e. , by chains adsorbed on surface "1" with or without forming bridges. Therefore, an expression can be written for the average number of loops on surface "1" per bridging chain, $n^{b}_{1,l}$ as explained in Schuetjens and Fleer's paper.[12] The average size of such loops can be calculated using an expression similar to eq 39. The average number of loops on surface "1" per unit area, n_l, is then given by

$$n_l = \frac{n}{L}\{n^{a}_{1,l} f^{a}_{1} + n^{b}_{1,l} f^{b}_{1}\} \tag{42}$$

where f^{a}_{1} is the fraction of chains adsorbed on surface "1" and f^{b}_{1} is the fraction of bridging chains with the last chain end leaving from surface "1", and they are given by

$$f_1{}^{a} = \frac{\theta^{a}_{1}}{\sum_z \phi(z)} \tag{43}$$

$$f^{b}_{1} = \frac{\theta^{b}_{1}}{\sum_z \phi(z)} \tag{44}$$

The average size of loops adsorbed on surface "1" $l_{1,l}$ is then obtained as a weighted sum of the two average sizes $l^{a}_{1,l}$ and $l^{b}_{1,l}$, and is given by

$$l_{1,l} = \frac{l^{a}_{1,l} n^{a}_{1,l} f^{a}_{1} + l^{b}_{1,l} n^{b}_{1,l} f^{b}_{1}}{n^{a}_{1,l} f^{a}_{1} + n^{b}_{1,l} f^{b}_{1}} \tag{45}$$

2.5. Estimation of Interaction Forces. In this section, we briefly outline how to calculate the force of compression of two interacting polymer layers. While the free energy of the system is given by the logarithm of the partition function[25] considered, the calculation of interaction forces does *not* follow directly from the derivative of free energy. We present only a brief summary of the needed equations here. A detailed derivation of the thermodynamics and the calculation of forces will be discussed in a future publication.

Under full equilibrium conditions, each layer parallel to the surface, z, is in thermodynamic equilibrium with its adjacent layer and with the bulk solution. Because of the presence of the surfaces, there is an inhomogeneity in the segment concentration along z and accompanying variations in the local pressure (stress) and the local generalized chemical potential. The conditions for thermodynamic equilibrium are the constancy of the pressure-corrected generalized chemical potentials of the solvent and the polymer segment in each layer and in the bulk. They are given by the equations

$$\mu^{0,g}(z) + v^{0}\Pi(z) = \mu^{0,b} + v^{0}\Pi^{b} \tag{46}$$

and

$$\frac{\mu^{g}(z)}{r} + v\Pi(z) = \frac{\mu^{b}}{r} + v\Pi^{b} \tag{47}$$

where $\mu^{0,g}(z)$ and $\mu^{g}(z)$ are the generalized chemical potentials of the solvent and polymer, v^0 and v are the volume occupied by a solvent molecule and a polymer segment ($v^0 = v = 1$), and $\Pi(z)$ and Π^b are the local and the bulk osmotic pressures. When the two surfaces interact (i.e., force is nonzero), external work has to be performed to keep them at their specified locations. Therefore, the force of compression can be viewed as a disjoining pressure of a thin polymer film. From an analogy to thin liquid films,[26] and from other works on this problem,[27,28] the force under full equilibrium conditions is found to be the excess normal stress in the system,

$$f = \Pi_m - \Pi^{b} \tag{48}$$

where Π_m is the osmotic pressure (isotropic stress) at the midpoint.

The restricted equilibrium situation corresponds to a system which is open with respect to solvent molecules but closed with respect to polymer chains and is represented by a semigrand ensemble. It is intuitive to consider this system as a grand canonical ensemble with an appropriate Lagrange multiplier $g(z)$ to maintain the fixed number of polymer chains in the system. Then the conditions for thermodynamic equilibrium are given by

$$\mu^{0,g}(z) + v^{0}\Pi(z) = \mu^{0,b} + v^{0}\Pi^{b} \tag{49}$$

and

$$\frac{\mu^{g}(z)}{r} + g(z) + v\Pi(z) = \frac{\mu^{b}}{r} + v\Pi^{b} \tag{50}$$

The Lagrange multiplier is identically equal to zero for the solvent. Under these conditions, one contends with an additional deviatoric stress in the system that accounts for the constancy of the number of polymer chains in the system. The expression for the force is then given by[27,28]

$$f = \Pi_m - \Pi^{b} - 2g_m\phi_m \tag{51}$$

where $(\Pi_m - \Pi^b)$ is the excess isotropic stress in the system, and $-2g_m\phi_m$ is the deviatoric correction to the force, g_m and ϕ_m being the Lagrange multiplier and the polymer volume fraction, respectively, at the midpoint. However, Scheutjens and Fleer[12] approximate the restricted equilibrium problem to an equivalent full equilibrium problem with an appropriate closure condition (e.g., the total amount of polymer in the interface is held constant in the restricted equilibrium situation). This essentially means that eq 50 becomes

$$\frac{\mu^{g}(z)}{r} + v\Pi(z) = \frac{\mu^{b}_{eff}}{r} + v\Pi^{b}_{eff} = \frac{\mu^{b}}{r} + v\Pi^{b} - \hat{g} \tag{52}$$

where μ^{b}_{eff} and Π^{b}_{eff} are the chemical potential of the

Table 1. Segment Density Distribution of Loops, Tails, Trains, and Bridges for $\Gamma = 0.75$, $H/a = 5.0$, $r = 200$, and $\chi_s = 1.0k_BT$

	overall segment density			tail segment density			bridge segment density			loop segment density		
layer	simulations	SCAFT	SF_2	simulations	SCAFT	SF_2	simulations	SCAFT	SF_2	simulations	SCAFT	SF_2
1	0.543	0.542	0.485	0	0	0	0	0	0	0	0	0
2	0.160	0.160	0.199	0.0071	0.0073	0.0086	0.050	0.040	0.055	0.104	0.114	0.136
3	0.093	0.090	0.132	0.0061	0.0065	0.0087	0.054	0.045	0.065	0.033	0.038	0.058
4	0.160	0.160	0.199	0.0071	0.0073	0.0086	0.049	0.040	0.055	0.104	0.114	0.136
5	0.544	0.542	0.485	0	0	0	0	0	0	0	0	0

polymer chain and the osmotic pressure corresponding to an "effective" bulk solution. Thus, the effective-full-equilibrium approximation leads to $\hat{g}$, an effective additional potential or stress needed per segment. Then eq 51 is replaced by

$$f = \Pi_m - \Pi^b - 2\hat{g}\phi_m \tag{53}$$

The chemical potentials and the osmotic pressures in eqs 52 and 53 are evaluated within the Flory−Huggins approximation for each layer.[13]

3. Results and Discussion

We shall now examine what changes or improvements one observes concerning the structure of the adsorbed layers and the forces resulting from the interaction between two adsorbing (polymer-bearing) surfaces when anisotropy is introduced in the mean-field formalism. Our primary focus here will be on the results of SCAFT-SF_2 relative to its isotropic version, SF_2. The structure and isotropic stresses in the system can also be obtained exactly using simulations, as we have discussed elsewhere.[21] We shall compare the predictions of the structure of adsorbed layer by SCAFT-SF_2 and SF_2 with some simulation results. The simulation results used in the following discussion are based on a lattice Monte Carlo technique in which we model the polymer chains as self-avoiding walks (SAW's) and sample the chain statistics using a modification of the configurational bias algorithm of Siepmann and Frenkel[29] due to de Joannis.[30] We use periodic boundary conditions in the x and y directions and consider two impenetrable, adsorbing surfaces confining the layers in the z-direction. The surface/segment interaction is considered only in the adjacent layer, as shown in eq 5. All results have been generated for chains of 200 segments, in a good solvent with a simple-cubic lattice of size $L/a = 40$ in the x and y directions,[31] where a is the lattice spacing.

In the present paper, we focus on the introduction of anisotropy in the mean-field theory and attempt to understand what improvement it offers. An attempt is made to relate the force between the two adsorbing surfaces to the structure of the adsorbed layers.

3.1. Structure of the Adsorbed Layers. We first focus on the overall segment density distribution. Segment densities are reported, following the normal convention, as the fraction of a lattice layer occupied by segments (i.e., area fraction). As an example, Figure 2 presents the overall segment density for the case of surface coverage $\Gamma = 0.75$ and $H/a = 5.0$ (Figure 2a) and for $\Gamma = 1.0$ and $H/a = 40$ (Figure 2b). The predictions of SF_1 (i.e., based on the first-order Markov statistics for the chains) are also shown in Figure 2, parts a and b. The corresponding segment densities of loops, tails, trains, and bridges for $\Gamma = 0.75$ and $H/a = 5.0$ are given in Table 1. Some more results on the overall segment densities and segment densities of loops, tails, trains, and bridges are available in the Supporting Information in Table 1s for different surface separations and surface coverages.

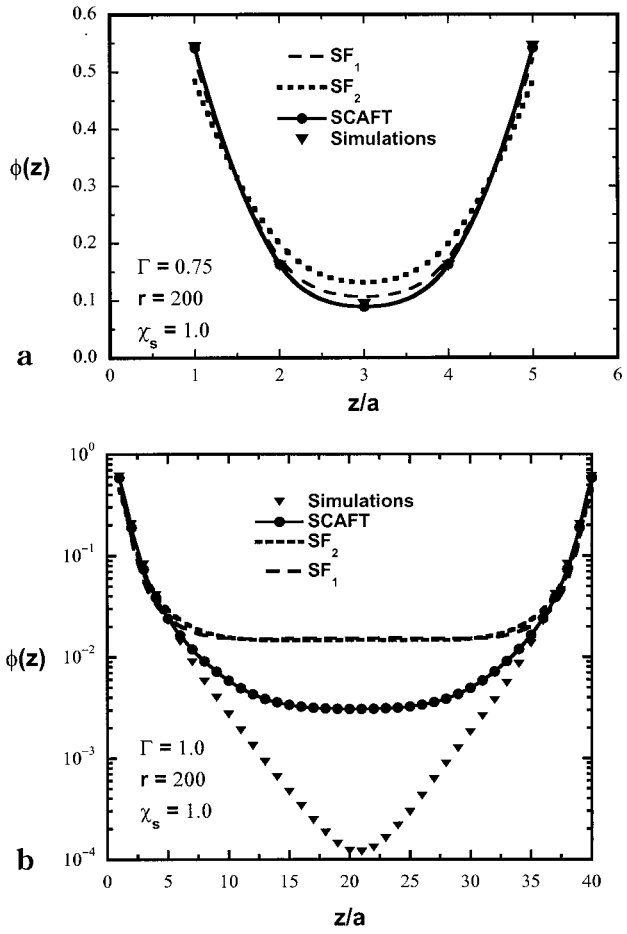

Figure 2. Overall segment density distribution: (a) $H/a = 5.0$; (b) $H/a = 40.0$.

On the basis of the above results, first one observes that, for $H/a = 5.0$, while the predictions of the overall segment density of SF_1 agree well with the simulations, those of SF_2 differ consistently. Since SF_2 prevents segment backfolding, it permits a lower number of allowable conformations near the surface than SF_1, which results in reduced segment densities near the surface (where the concentration is high) and higher value of densities away from the surface. This results in SF_2 predicting higher segment densities for the bridges, loops, and tails and lower densities for trains as compared to SF_1 and simulations. Introduction of anisotropy significantly improves the predictions. SCAFT partially corrects SF_2 in the appropriate manner. The overall segment density profiles show a surprising agreement with the simulations for $H/a = 5.0$. However, for $H/a = 40.0$, it is clear that the corrections due to anisotropy are insufficient to capture the interactions

between the segments accurately. Even SCAFT predicts an order of magnitude higher segment densities near the center.

In general, the correction due to anisotropy in the mean field is two-fold.

(1) Near the Surface. In typical situations near an adsorbing surface one would expect a significant density of trains under strongly adsorbing conditions (i.e., $\phi(z = 1)$) in which all segments are oriented in the same direction (*i.e.*, parallel to the surface). Introduction of anisotropy will cause more bonds to orient along the surface, thus giving rise to an increase in the number of segments forming trains. This is confirmed by the increase of segment densities of trains (relative to SF_2) observed in Figure 2, parts a and b. This improvement also gives rise to an excellent agreement between SCAFT and simulations in the overall segment density near the surface.

(2) Far from the Surface. Anisotropy also leads to an underprediction of the segment density of bridges compared to SF_2 and simulations. Far from the adsorbing surfaces, the bond orientations are almost random, and hence, the introduction of anisotropy (ordering) only serves to increase the "rigidity" of the chain, i.e., decrease the number of allowable conformations for that part of the chain, resulting in a lower density compared to isotropic mean-field predictions. Further, restricted equilibrium requires that the total amount of polymer chains between the surfaces remain constant. Therefore, an increase in the segment density near the surface will have to be accompanied by a corresponding decrease away from the surface.

SCAFT also predicts lower segment densities of tails and loops[32] relative to SF_2 but higher values compared to the simulations. Again, one observes that the correction due to anisotropy leads to an improvement but the results still differ from those of the simulations possibly because of the mean-field approximation in the introduction of anisotropy. The results obtained for the number and size of bridges, loops and tails confirm the above observations. Sample results are shown in Figure 3, parts a and b, for the number and size of bridges (for $\Gamma = 0.75$). Further results for the number and size of bridges, loops and tails as functions of Γ and H/a are avaiable as Supporting Information (Figures 1s−10s). SCAFT predicts lower number of bridges than SF_2 and simulations, but bridges of larger average size than the simulations. This difference is pronounced at larger separation distances. The net result is an underprediction of the segment densities contributed by bridges.

3.2. Interaction Forces. One of the central issues that is not clearly understood is the relationship between the structure of the adsorbed layer and the resulting forces of interaction between two adsorbed layers. Evidently, the work done in compressing two layers (and hence the interaction force) depends on the rearrangement of the bridges, loops, tails, and trains upon compression. While bridges generally contribute to an attractive interaction between the surfaces, interactions among tails, bridges, and loops result in steric repulsion. It is of interest to examine the effects of bond correlations on the balance between the two competing factors in determining the interaction between two adsorbed layers. Further, as noted earlier, an evaluation of the performance of mean-field approximations would be incomplete without an examination of the forces of compression due to the interaction between two layers.

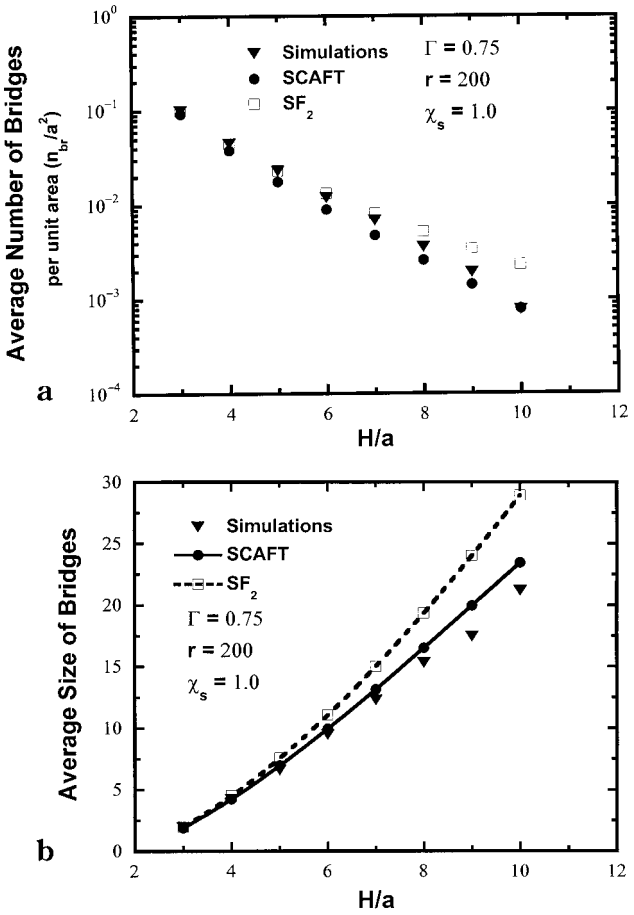

Figure 3. Number and size distribution of bridges, as a function of H/a, for a constant adsorption energy, $\chi_s = 1.0\ k_BT$ and $\Gamma = 0.75$; (a) average number of bridges, n_{br}; (b) average size of bridges, l_{br}.

Here, we shall consider the effect of the introduction of anisotropy in the mean field on polymer-induced forces.

At low surface coverages, one essentially encounters a single-chain regime. Therefore, the system can be analyzed as a collection of single chains. When the surfaces are close to each other, at strong adsorption conditions, the chains form bridges between the surfaces. These bridges are loosely stretched, and as a first approximation, can be considered to behave as Hookean springs.[33] As the surface separation increases, the bridges become strongly stretched, and then one can consider the system to be a collection of nonlinear elastic tethers,[34] with each tether governed by the Pincus law of elasticity.[35] In this single-chain regime, the interaction between the two surfaces is predominantly attractive, with the exception of very low separations, where steric interactions between the segments of the chain lower the attraction. As the surface coverage increases, the chains are packed closer and closer that beyond the proximal regions of the layers, the system is in a semidilute regime, and steric interactions between different sections of a chain and between chains become important. Under such conditions, the force of interaction between the surfaces crosses over from attraction to repulsion. Such behavior has also been qualitatively observed in experiments (see for instance, Fleer et al.[13]).

Scheutjens and Fleer[12] have examined this problem in the lattice mean-field approximation and have been able to reproduce the bridging-attraction and steric-repulsion force profile qualitatively. They used the first-

order Markov approximation to model the chains in the lattice (SF_1). What is surprising about their results is that the mean-field theory appears to provide reasonable predictions in the single-chain regime, which is counterintuitive. As mentioned toward the end of section 2.5, we shall discuss the correct calculation of forces of compression using lattice mean-field theory, and reinterpret the Scheutjens−Fleer results in another manuscript. Here, we show that even with the introduction of anisotropy in the mean field, the lattice mean-field theory fails to capture any significant bridging attraction. We shall restrict our discussions to the effects of polymer layer anisotropy on the predictions of force of compression of the polymer layers.

We first examine the force per unit area (the excess normal stress in the system) as a function of surface separation H/a, for surface coverages $\Gamma = 0.25$ through 1.25, and for an adsorption energy $\chi_s = 1.0k_BT$, in Figure 4, parts a−c. For the extent of bridging observed at the conditions examined (see for instance Figure 3, parts a and b, and Figure 1s in Supporting Information), the observed attraction at low coverages is nearly negligible. We shall revisit this observation toward the end of this section and draw further conclusions. An interesting observation to be made from these figures is that at high coverages, SCAFT and SF_2 predict a repulsive force with a power law behavior, the exponent being independent of the coverage. The exponents are −3.67 and −3 for SCAFT and SF_2, respectively.

To further illustrate and understand the limitations of mean-field theories, we examine the force as a function of Γ for a fixed surface separation $H/a = 4.5$, shown in Figure 5a. The results of SF_1 (with the correct calculation of forces) are also included for comparison. It is clear that at low coverages, there is seldom any attraction predicted by any of the mean-field formulations. At high coverages, we observe that SF_2 predicts higher repulsion than SCAFT. This is counterintuitive, since the introduction of anisotropy serves to increase the "rigidity" of the chains. For this reason, one would expect a polymer layer in an anisotropic mean-field to be less compressible than one in isotropic mean field. However, mean-field theories underestimate the saturation coverage[36] due to the fact that the excluded-volume interactions are implemented in a mean-field sense and that the chain statistics permit overlap and crossover. It is found that the saturation coverages for simulations,[37] SF_1, SF_2, and SCAFT are, respectively, 1.2, 0.7, 0.72, and 0.92. This explains why SF_2 predicts less compressible layers than SCAFT, contrary to intuition.

Moreover, due to the differences in the chain statistics and the mean-field assumptions, one can expect that the critical adsorption energy[38] χ_c will be different for the different approximations, namely, SF_1, SF_2, and SCAFT and SAW simulations.[37] Our calculations show that the critical adsorption energies are, respectively, 0.18, 0.22, 0.21, and 0.26. Due to the differences in Γ_0 and χ_c, it is instructive to examine the results for the same relative surface saturation and relative adsorption energies. Therefore, we plot the force per unit area as a function of rescaled coverage Γ/Γ_0 for a fixed H/a and a rescaled adsorption energy $(\chi_s - \chi_c)$ in Figure 5b. The results are similar to those shown in Figure 5a, except that, at high coverages, SCAFT is now seen to predict higher repulsive forces, as would be expected. The average number and size of bridges, loops and tails are plotted as a function of Γ/Γ_0 for a given $(\chi_s - \chi_c)$. Figure 6, parts a and b, show the number and size of bridges. The number and size of loops and tails are available in the Supporting Information (see Figures 11s−14s).

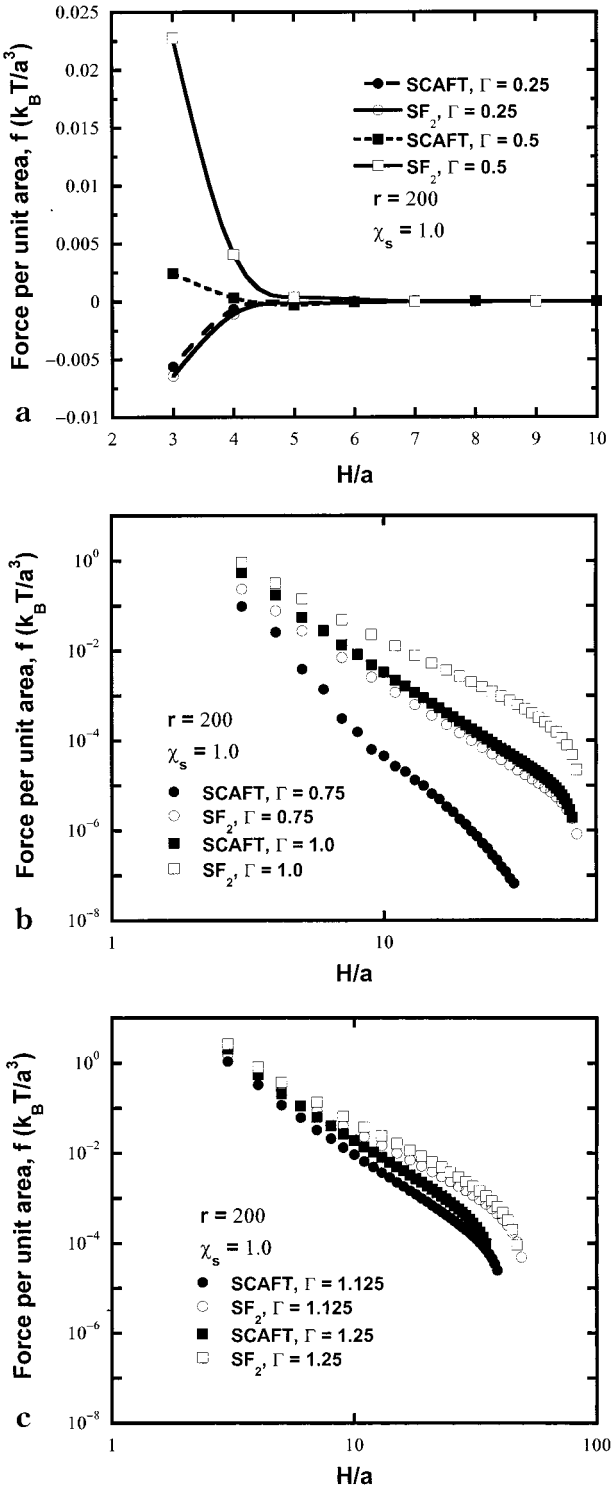

Figure 4. Force per unit area between the surfaces f as a function of surface separation H/a: (a) $\Gamma = 0.25$, 0.5; (b) $\Gamma = 0.75$, 1.0; (c) $\Gamma = 1.125$, 1.25.

An enlarged view of the results at low coverages, illustrated in Figures 4a, 5a, and 5b, shows that SCAFT and SF_2 do predict some attraction, even though quantitatively negligible. As stated earlier, in a highly undersaturated regime, the chain conformations are dicated essentially by single-chain statistics. The assumption of mean-field is expected to be highly inac-

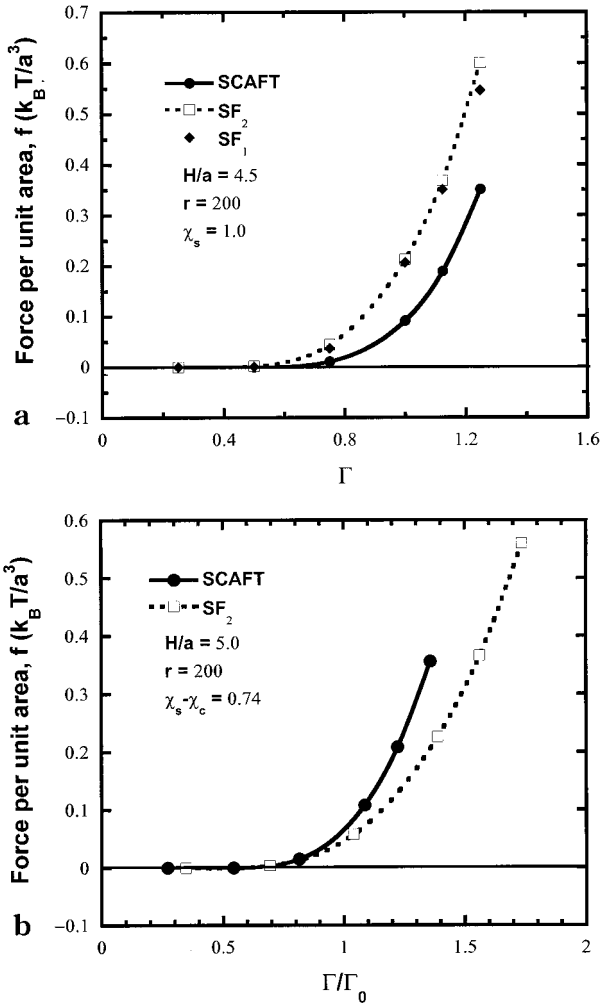

Figure 5. Force per unit area f at a fixed separation of $H/a = 4.5$: (a) as a function of surface coverage Γ, for adsorption energy $\chi_s = 1.0\ k_BT$; (b) as a function of rescaled surface coverage Γ/Γ_0, for rescaled adsorption energy $\chi_s - \chi_c = 0.74$.

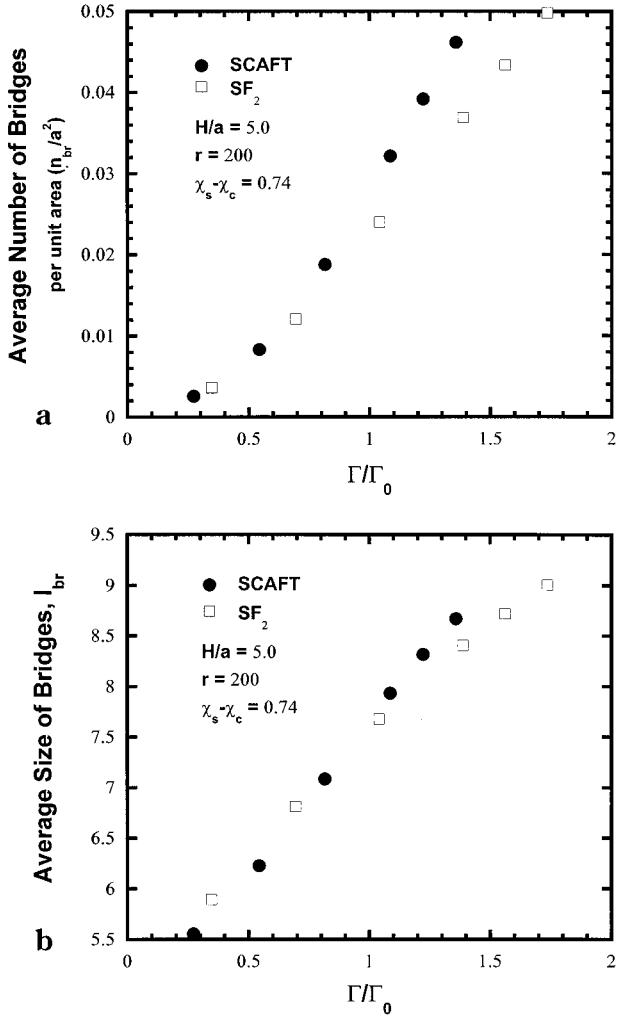

Figure 6. Number and size distribution of bridges, as a function of rescaled surface coverage Γ/Γ_0, for a constant rescaled adsorption energy, $\chi_s - \chi_c = 0.74$, and $H/a = 5.0$: (a) average number of bridges, n_{br}; (b) average size of bridges, l_{br}.

curate here. For chains in a lattice, constructed with a first-order Markov statistics, with random mixing approximation in the lateral dimensions, the following expression has been used[11] to estimate the radius of gyration R_g, expressed as a multiple of the length of a step in the lattice,

$$R_g^2 = (r/6)(1 + D^{-1})(1 - D^{-1}) \qquad (54)$$

where r is the chain length, and D is the lattice coordination number. For a chain length of 200 segments in a cubic lattice, the radius of gyration is about 5.7 lattice units. On the basis of the estimates of *rms* thickness of the adsorbed layer, one can estimate that single-chain statistics prevails up to a surface coverage of $\Gamma \sim 0.5$. Therefore, the observed attraction then corresponds to that of an ideal nonreversal chain (SF_2), and a weighted ideal nonreversal random walk (SCAFT). We noted earlier that at low coverages the system is expected to behave as a collection of single bridges with negligible interactions among bridges. Therefore, the magnitude of the attractive force is expected to increase linearly with surface coverage. The number of bridges in this regime decreases exponentially and the length of the bridges increases linearly[39] with H/a. To see if the system behaves as a collection of elastic tethers

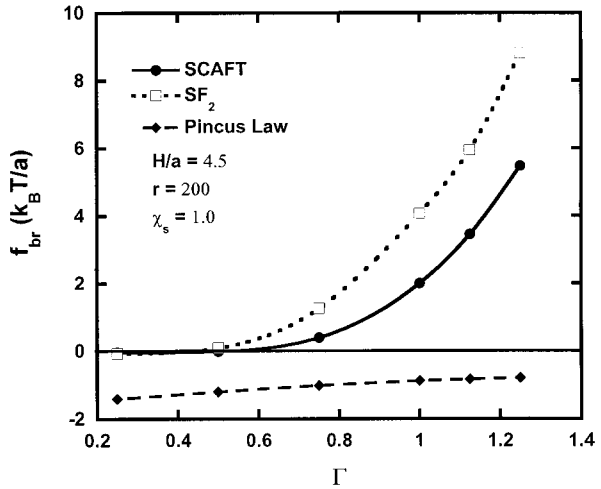

Figure 7. Force per bridge f_{br} as a function of Γ for a fixed wall separation $H/a = 4.5$.

(governed by Pincus law of elasticity[35]) in the strongly stretched region, we plot the force *per bridge* as a function of Γ in Figure 7. At very low coverages, one does observe a qualitatively similar behavior, though the magnitude of the force is much less than the Pincus law estimate.

The preceding observations indicate that the mean-field theories are severely limited in their ability to provide a reasonable quantitative estimate of the attraction between interacting polymer layers at low coverages, under restricted equilibrium. They predict qualitatively expected behavior at higher coverages, where steric interactions are significant. The attempt to improve mean-field predictions by the introduction of anisotropy seems to work in the prediction of structural details of the adsorbed layer but is clearly wanting in the prediction of forces. To obtain any significant improvement in the predictions of the theories of polymer adsorption, one may have to go beyond the constraints of the mean field. Further, inadequate chain statistics (which one often resorts to in order to retain manageable propagation relations) introduce further limitations in the theoretical predictions. Even though the elimination of backfolding leads to a significant improvement, as shown in this work and by Jimenez et al.[21] and Simon and Ploehn,[40] this is merely the simplest of the refinements that may be necessary. A careful examination is needed to study the limitations due to chain statistics.

4. Closing Remarks

In summary, we have presented an examination of the effects of the orientational anisotropy of polymer chains in a physisorbed layer on mean-field predictions of structure of the layer and the resulting forces of interactions between two layers. In addition to chain statistics, anisotropic effects are expected to be among the most important elements of mean-field theories having an impact on the predictions. Our objective here has been to present at least a preliminary examination of what improvements can be expected through the introduction of anisotropy.

The results show that introduction of anisotropy does improve the segment density distribution close to the adsorbing surface. However, far away from the surface, mean-field theories consistently predict higher densities than simulations. It is also found that mean-field theories fail to provide useful results at lower coverages on the forces of interaction. A linear force profile, qualitatively consistent with the scaling predictions of Ji et al.,[34] is observed at low surface coverages, even though there are quantitative discrepancies. Both the mean-field formulations predict the crossover from net attraction to repulsion to occur at similar coverages ($\Gamma/\Gamma_0 \sim 0.5$).

In the above comparisons, we have used the structural properties computed using Monte Carlo simulations as a reference. However, a caveat is in order in this respect, namely that there is no clear way to compare rigorously the mean-field theories with exact calculations (e.g., simulations). To be able to make any conclusive comments on the reliability of mean-field theories even for the simple problem of homopolymer adsorption, one has to consider many issues. First, an agreement between a mean-field formulation (e.g., SF_1) and simulations for only certain properties (e.g., segment densities) does not necessarily imply that the formulation will be equally good for all properties. Second, the fact that improving the chain statistics leads to improved segment densities in certain regions (as we noted in the previous section) does not guarantee that similar improvements can be expected in the overall performance. That is, agreement in certain respects could occur because of fortuitous cancellation of errors, while the errors could compound each other in other respects. Third, it is unclear currently as to what is the right way (or the best way) to compare mean-field calculations with simulations. Intuitively, it appears reasonable to compare the results for the same rescaled coverage, Γ/Γ_0, and rescaled adsorption energy, $(\chi_s - \chi_c)$. However, whether such a rescaling is sufficient (or even valid) remains unclear. This issue deserves further attention, since the interpretations could be misleading if the right comparisons are not made. On the other hand, despite such uncertainties, the use of simulations as benchmarks remains the only option to examine the reliability of the mean-field theories, since a direct comparison with experiments only introduces additional uncertainties. We hope to comment on some of these issues in a future publication.

Supporting Information Available: Table giving the segment density distribution and figures giving average numbers and sizes of bridges, loops, and tails as a function of surface coverage, H/a, and rescaled surface coverage. This material is available free of charge via the Internet at http://pubs.acs.org.

References and Notes

(1) de Gennes, P.-G. *Scaling Concepts in Polymer Physics*; Cornell University Press: Ithaca, NY, 1979.

(2) Edwards, S. F. *Proc. Phys. Soc.* **1965**, 85, 613.

(3) de Gennes, P.-G. *Macromolecules* **1981**, 14, 1637.

(4) de Gennes, P.-G. *Macromolecules* **1982**, 15, 492.

(5) Dolan, A. K.; Edwards, S. F. *Proc. R. Soc. (London) A* **1975**, 343, 427.

(6) Semenov, A. N.; Joanny, J.-F. *Europhys. Lett.* **1995**, 29, 279.

(7) Semenov, A. N.; Bonet-Avalos, J.; Johner, A.; Joanny, J.-F. *Macromolecules* **1996**, 29, 2179.

(8) Bonet Avalos, J.; Joanny, J.-F.; Johner, A.; Semenov, A. N. *Europhys. Lett.* **1996**, 35, 97.

(9) Mendez-Alcaraz, J. M.; Johner, A.; Joanny, J.-F. *Macromolecules* **1998**, 31, 8297.

(10) Scheutjens, J. M. H. M.; Fleer, G. J. *J. Phys. Chem.* **1979**, 83, 1619.

(11) Scheutjens, J. M. H. M.; Fleer, G. J. *J. Phys. Chem.* **1980**, 84, 178.

(12) Scheutjens, J. M. H. M.; Fleer, G. J. *Macromolecules* **1985**, 18, 1882.

(13) Fleer, G. J.; Cohen Stuart, M. A.; Scheutjens, J. M. H. M.; Cosgrove, T.; Vincent, B. *Polymers at Interfaces*; Chapman & Hall: London, U.K., 1993.

(14) Klein, J.; Rossi, G. *Macromolecules* **1998**, 31, 1979.

(15) Jones, I. S.; Richmond, P. *J. Chem. Soc., Faraday Trans. 2* **1977**, 73, 1062.

(16) Leermakers, F. A. M.; Scheutjens, J. M. H. M.; Gaylord, R. J. *Polymer* **1984**, 25, 1577.

(17) Leermakers, F. A. M.; Scheutjens, J. M. H. M. *J. Chem. Phys.* **1988**, 89, 6912.

(18) van der Linden, C. C.; Leermakers, F. A. M.; Fleer, G. J. *Macromolecules* **1996**, 29, 1172.

(19) Fleer, G. J.; van Male, J.; Johner, A. *Macromolecules* **1999**, 32, 825.

(20) Fleer, G. J.; van Male, J.; Johner, A. *Macromolecules* **1999**, 32, 845.

(21) Jimenez, J.; de Joannis, J.; Bitsanis, I.; Rajagopalan, R. *Macromolecules* **2000**, 33, 8512.

(22) Notice that the correction to the mean field is independent of the chain statistics used (in this case, a second-order Markov statistics).

(23) We call this the *statistical weight* for obvious reasons.

(24) We use the approach of Scheutjens and Fleer[12] here.

(25) The expression is given in Scheutjens and Fleer's paper.[12]

$$\frac{(F - F^0)}{Lk_BT} = \frac{\theta^t}{r}\ln\frac{\theta^t}{G(r)} + \sum_{z=1}^{M}\ln(1-\phi(z)) + \chi\sum_{z=1}^{M}\phi(z)\langle\phi(z)\rangle - \mu^0\frac{(M-\theta^t)}{k_BT} \quad (55)$$

Here, F^0 is the free energy of pure solvent between the surfaces. For an incompressible system, this free energy corresponds to the Helmholtz free energy.

(26) de Feijter J. A.; Rijnbout, J. B.; Vrij, A. *J. Colloid Interface Sci.* **1978**, *64*, 258.

(27) Evans, E. *Macromolecules* **1989**, 22, 2277.

(28) Ploehn, H. J. *Macromolecules* **1994**, *27*, 1627.

(29) Siepmann, J. I.; Frenkel, D. *Mol. Phys.* **1992**, 75, 59.

(30) de Joannis, J. Ph.D. Dissertation, University of Florida, Gainesville, FL, 2000.

(31) The numerical mean-field theories considered here are one-dimensional; i.e., the *x* and *y* directions extend to infinity and variations in segments densities are considered only in the *z* direction. Hence in the mean-field context, the lattice size of $(L/a) = 40$ specified in the *x* and *y* directions simply implies that 1600 lattice sites are considered per layer.

(32) This could explain why SCAFT predicts lower repulsion than SF_2 in Figure 5a.

(33) Jimenez, J., de Joannis, J.; Bitsanis, I.; Rajagopalan, R. *Macromolecules* **2000**, 33, 7157. In this work, the distribution of bridges and snapshots from simulations have been shown for a single chain of 1000 segments, to illustrate the importance of bridge−bridge steric interactions, especially at weak adsoprtion energies, and how such interactions play a vital role in systems with multiple chains.

(34) Ji, H.; Hone, D.; Pincus, P.; Rossi, G. *Macromolecules* **1990**, 23, 698.

(35) Pincus, P. *Macromolecules* **1976**, 9, 386.

(36) The saturation coverage Γ_0 is defined as the limiting value of Γ corresponding to $\phi_b \rightarrow 0$. For short chains, Γ_0 is obtained from the adsorption isotherm (a plot of Γ^* as a function of ϕ_b) from an extraploation of the equilibrium coverage Γ^* (beyond the initial rise) to $\phi_b = 0$.

(37) de Joannis, J.; Park, C.-W.; Thomatos, J.; Bitsanis, I. *Langmuir* **2001**, 17, 69.

(38) The *critical adsorption energy* χ_c is the effective adsorption energy for which the energetic attraction of the segments to the surface is compensated exactly by the entropic repulsion arising from the conformational restrictions imposed by the presence of surface. Therefore, at $\chi_s = \chi_c$, the overall segment density profile is flat. The critical adsorption energy is estimated as the adsorption energy at which the surface excess θ^{exec} $(= \sum_z(\phi(z) - \phi_b)$, where ϕ_b is the bulk concentration) is zero.[18.]

(39) This type of behavior has been suggested by Ji et al.,[34] who show that the elasticity of such strongly stretched tethers is nonlinear and is governed by what is known as the Pincus law of elasticity.[35.]

(40) Simon, P. P.; Ploehn, H. J. *Macromolecules* **1998**, 31, 5880.

MA011395P